Received: 20 December 2019 | Revised: 26 March 2020 | Accepted: 31 March 2020

DOI: 10.1002/pc.25600

Check for updates

RESEARCH ARTICLE

Polymer COMPOSITES WILEY

Structural and tensile characteristics of reduced graphene oxide/poly (vinyl alcohol) composite films: Influence of ultraviolet irradiation

Altan Bozdoğan[1] | **Baki Aksakal**[1] | **Onder Yargi**[1] | **Utkan Şahintürk**[2]

[1]Department of Physics, Faculty of Arts and Sciences, Yıldız Technical University, İstanbul, Turkey

[2]Department of Mechanical and Metal Technology, Vocational School of Technical Sciences, İstanbul University-Cerrahpasa, İstanbul, Turkey

Correspondence
Altan Bozdoğan, Department of Physics, Faculty of Arts and Sciences, Yıldız Technical University, İstanbul 34210, Turkey.
Email: abozdog@yildiz.edu.tr

Funding information
Yıldız Technical University, Scientific Research Projects Coordinatorship, Grant/Award Number: 2016-01-01-GEP02

Abstract

The influence of ultraviolet (UV) radiation on the structural and uniaxial tensile characteristics of reduced graphene oxide (rGO)/poly(vinyl alcohol) (PVA) composite films produced by using various contents (0-10 wt%) of rGO obtained by a microwave-assisted reduction process was investigated. With increasing rGO content, significant reinforcing effects of the rGO sheets were seen on the tensile characteristics of the unirradiated rGO/PVA composite films, that is, increases in the stiffness and rigidity and decreases in the strain at break values. After UV exposure times from minutes up to 1 hour, for all the rGO contents, the rGO/PVA composite films had improved tensile strength and modulus values as well as considerable improvement in the stress-strain behavior in spite of great decreases in the strain at break values. The structural changes responsible for the improvement in the tensile strength and Young's modulus of the rGO/PVA composite films were associated with the development of strong intermolecular interactions between the rGO sheets and the PVA polymer chains through the formation of hydrogen bonds. Deterioration of the mechanical characteristics, especially strain at break values, was mainly due to the photodegradation of the structural units induced by UV radiation leading to the formation of some free radicals caused by the chemical bond breakages in the polymer chains as well as the weakening of intermolecular interactions such as hydrogen bonds. Correlation between the changes in the tensile properties and the structure of the rGO/PVA composite films were sought by analyzing tensile testing, fourier transform infrared/attenuated total reflectance (FTIR/ATR), and UV-visible spectral results.

KEYWORDS

FTIR, irradiation, mechanical properties, thin films, UV-vis spectroscopy

1 | INTRODUCTION

Graphene is composed of a single layer of carbon atoms in a two dimensional, honeycomb crystal lattice.[1,2] Two-dimensional graphene sheets are known as the strongest materials developed so far.[3,4] Because of its very low density and good mechanical properties, it has often been used as reinforcement material in polymer nanocomposites.[5–7] Due to high thermal and electrical conductivity as well as high tensile strength and

 © 2020 Society of Plastics Engineers

modulus, it has also been used for many applications based on carbon materials (carbon nanotubes).[8–10] It has also been used in solar cells,[11] sensors,[12] and supercapacitors applications.[13,14] As a graphene derivative, graphene oxide (GO) and reduced GO (rGO) have been widely studied for application in various fields, including energy devices,[15,16] conductive devices,[17] and polymer nanocomposites.[18,19] One of the polymer nanocomposites that have been produced is based on poly(vinyl alcohol) (PVA) with the addition rGO in order to improve the mechanical, electrical, and optical properties of the PVA material. PVA is known as a water soluble, biodegradable, synthetic polymer and is mostly used in the production of polarizer films[20] and in the textile[21] and food industries,[22] as well as the manufacture of paper products.[22] In the literature, although there are many studies of the mechanical, thermal, electrical conductivity, and the optical properties of PVA nanocomposite films with the addition of GO,[23–32] there are only a few studies that investigate the properties of rGO/PVA nanocomposite films. In one of them, at low rGO content (up to 3%), the thermal, mechanical, and structural properties were investigated and it was reported that with increasing rGO content the tensile strength and Young's modulus increased from 70 to 108 MPa and from 4 to 6 GPa, respectively. On the contrary, the tensile strain decreased dramatically, from about 78% to 9%.[1]

Because the nanocomposites based on PVA with the addition of rGO have potential applications in various fields, such as solar cells and sensors, which depend on their thermal, mechanical, and conductivity properties, the need for the determination of the influence of the ultraviolet radiation, such as UVA and UVB, on the mechanical, structural, and photodegradation properties of these nanocomposites is quite important to improve and optimize the properties of these composites when exposed to UV radiation for such different applications. In the literature, there are some studies investigating the effect of UV irradiation on the photodegradation and mechanical properties of only the pure PVA films.[20,33] In one of them,[20] it was reported that Young's modulus and tensile strength both increased by almost 1.5 times, while the strain at break did not change much after the samples were irradiated by UV light at 400 W for 5 minutes. It is known that, depending on the wavelength of the light, the resulting effects on the structure of the polymers can differ. It is stated[34] that the free radicals are formed after irradiation of many polymers with UV light, even with $\lambda > 3000$ A in vacuum. Moreover, it was mentioned[33] that irradiation with UV light of wavelength greater than 260 nm resulted only in main-chain degradation which can cause the formation of free radicals that can affect many properties of the polymer. Considering the effect of UV light on PVA, in the study of Rudko et al.,[35] it was stated that the UV light with the 266-nm wavelength is absorbed by PVA due to the presence of imperfections of the polymeric chain. In that study, it was mentioned that these defects are predominantly acetate residuals, because of incomplete hydrolysis of polyvinyl acetate used for PVA production. It was also stated that the excitation of macromolecules typically initiates various types of photo-activated reactions in polymers containing PVA, such as chain scission,[36,37] formation of chromophore groups and free radicals,[38–41] breaking of intermolecular bonds,[37] configurational transformations,[42] and so on.

Even though it is known that rGO has a great reinforcement effect on the mechanical properties of PVA, we know of no reports of how the UV radiation will affect the photodegradation and other properties of the PVA films reinforced with varying contents of rGO, such as mechanical properties, when the rGO/PVA composite films are exposed to UV irradiation for short or longer times. To our knowledge, there has also been no detailed study investigating the effect of UV irradiation on the mechanical, optical, and structural properties of rGO/PVA composite films and what the role and the contribution of the rGO content on the photo degradation process of these composites are. Thus, the present study was aimed at investigating mainly the influence of UV irradiation on the tensile, spectroscopic and optical properties of rGO/PVA nanocomposite films with increasing rGO content. Moreover, the correlation between the changes induced by UV radiation in the tensile characteristics of the composite films with the related structural changes were investigated in detail by using tensile testing and FTIR/ATR and UV-visible (vis) spectroscopy.

2 | EXPERIMENTAL

2.1 | Materials

2.1.1 | Preparation of rGO

In this work, the method of microwave assisted reduction of GO to rGO was used to prepare the rGO. GO was prepared from graphite powder (Alfa Aesar by Thermo Fisher Scientific Inc., Bridgewater Township, New Jersey, graphite flake, natural, −325 mesh, 99.8% metal basis) with the method given earlier,[43,44] and then a stock of GO suspension of 20 mg mL^{-1} was prepared by bath ultrasonication in distilled water for 2 hours. The pH value of the pure GO solution was measured as 2.60 with pH meter (Thermo Fisher Scientific Inc., Orion Star A211). A specific amount of hydrazine monohydrate (Sigma Aldrich Corp., Taufkirchen, Germany, hydrazine

monohydrate, N_2H_4, composition: 64%-65%, reagent grade, assay: 98%) was added to the GO solution for adjusting the pH value to 10.00. The ratio of N_2H_4/GO was equal to (135 μL 400 mg^{-1}). Afterward, the suspension was ultrasonicated for 5 minutes followed by the microwave-assisted reduction. The rGO material was prepared by reducing the GO during the microwave-assisted synthesis reactions carried out in a microwave accelerated reaction (reactor) system. The microwave irradiation was applied in a microwave oven with 1600 W power and 2450 MHz for a time of 5 minutes (CEM Corp., Stallings, North Carolina, Mars 5 Digestion Microwave System).

2.1.2 | Preparation of rGO-PVA films

The PVA used in the production of the rGO-PVA composite films was obtained from Boysan Co. (Boysan Co., Turkey). It was in powder form and white color and was water soluble with a pH value of around 4.5 to 6.5. The polyvinyl alcohol was prepared from >92% by wt. acetic acid ethenyl ester polymer with ethanol, <5% by wt. water, <3% by wt. sodium acetate anhydrous, and <1% by wt. methyl alcohol. In order to produce the rGO-PVA composite films, rGO-PVA suspensions with different ratios were prepared by adjusting the amount of rGO with respect to that of PVA from 1 wt% up to 10 wt% rGO. After preparation of the mixture suspensions by sonication and stirring procedures, 3 mL of the rGO-PVA suspensions of the different weight rGO ratios were each poured into rectangular plastic boxes with the dimension of 2.5 × 6 × 0.5 cm and left to dry completely at room conditions for 3 days.

2.2 | Experimental methods

2.2.1 | Tensile testing method

Uniaxial tensile tests of PVA and the prepared composite films were carried out by using a tensile testing machine LF plus (AMETEK Lloyd Instruments Ltd, Bognor Regis, UK). Tensile tests were performed according to ASTM D-882-02. In order to choose a strain rate of 0.5-1.0 mm min^{-1} which is suitable for the percent elongation at break being around 20 or more, proper initial grip separation and the rate of grip separation were adjusted. For example, in order to apply a strain rate of 1 mm min^{-1}, grip separation was chosen as 20 mm and the rate of grip separation was chosen as 20 mm min^{-1}, accordingly. The test specimens used in the tensile tests had the same width of 4 mm. The thicknesses of pure PVA films were measured by using a digital micrometer (Mitutoyo Corp., Kawasaki, Japan, no. 293-821-30). The data reported here were averaged over at least six to eight specimens. In order to investigate the influence of UV irradiation on the stress-strain behavior of the PVA and rGO-PVA composites the films were irradiated for various times from 0.5 to 2 hours. Then, the unexposed and exposed films were tested by using the tensile tester at ambient temperature.

2.2.2 | UV irradiation method

Prior to the mechanical and spectral tests, all the films having the various rGO weight ratios from 0% to 10% were placed in a metal UV chamber. Before the irradiation, each rectangular sample was cut into smaller ones with the size of 4 mm × 60 mm and stuck on thin glasses from the ends in order to hinder bending or deformation of the samples during the irradiation process. The samples were irradiated with a self-ballasted UVA/UVB florescent lamp (OSRAM GmbH, Germany, Ultra Vitalux 300 W 230 V E27) with output power of 300 W, after being placed and focused at a distance of 40 cm in vertical direction from the UV lamp for each desired exposure time from 30 minutes to 2 hours. The UV lamp emitted UVA (315-400 nm) and UVB (280-315 nm) radiations with radiated powers of 13.6 and 3 W, respectively. Because the temperature of the metal UV chamber rose about 40°C to 50°C during the irradiation process, the specimens were left to cool down at room conditions after removal from the chamber.

2.2.3 | FTIR/ATR spectroscopic method

The FTIR/ATR spectroscopic measurements were conducted on a Thermo Scientific Nicolet iS5 (Thermo Fisher Scientific Inc.) FTIR spectrometer equipped with a iD7 ATR sampling accessory. The spectra of the samples before and after UV irradiation for various times were recorded in the wavenumbers range from 4000 to 400 cm^{-1} at a resolution of 4 cm^{-1} with 32 scans for each measurement at room conditions.

2.2.4 | UV-vis spectroscopic measurements

UV-vis absorption spectra of both unirradiated and irradiated films were measured in a spectrophotometer (Agilent Technologies Inc., Wilmington, DE, Agilent 8453 UV-vis spectrophotometer) in the

wavelengths ranging from 190 to 1100 nm at ambient temperature.

3 | RESULTS AND DISCUSSION

3.1 | Mechanical property analysis

The changes in the uniaxial tensile characteristics of unexposed pure PVA and rGO-doped PVA composite films with increasing rGO content are tabulated in Table 1. Young's modulus, E_Y, of the pure PVA was ca. 50 MPa and increased significantly as the rGO content was increased up to 10 wt%; an increase by a factor of 22 was observed. We suggest this significant increase was due to the rGO sheets dispersed homogeneously in the PVA polymer matrix with strong interfacial interactions between both components.

On the other hand, the tensile strength, σ_T, increased slightly for the low rGO contents, up to 2.5 wt%, and then decreased. Contrary to the significant improvement in Young's modulus, the strain at break values decreased slightly up to 2.5 wt%, and then decreased greatly with increasing rGO doping ratio. For a low content of rGO, that is, 1 wt%, the work or energy value to break the sample increased greatly when compared with that of pure PVA films, but then it decreased with further increase in rGO content which implies a change of the PVA structure to a more rigid structure. Considering the changes in the tensile characteristics of the rGO-PVA composite films, it should be noted that because graphene nanosheets are strong and rigid units, the distribution of these units in the PVA matrix improved the mechanical properties, such as stiffness and rigidity, due to the presence of the intermolecular interactions, such as hydrogen bonding between oxygen-containing moieties such as carbonyl, carboxyl, hydroxyl, ether, and epoxy groups, on the surfaces of the rGO sheets and the OH groups of the PVA polymer chains in contact with the rGO surfaces. Thus, because of the increasing rigidity, the elongation at break of the composite films decreased with increasing rGO content. However, with excess rGO loading, that is, 10%, the brittleness of the rGO/PVA nanocomposites increased, we assume that the extra added rGO sheets formed large rGO agglomerates of stacked rGO sheets by the van der Waals forces between them.

In order to investigate the influence of UV irradiation on the tensile characteristics of the pure PVA films, they were irradiated by the UV lamp for various times from 0 to 2 hours. The stress-strain curves of pure PVA exposed to UV irradiation for various times are shown in Figure 1, with the mechanical properties listed in Table 2; as the UV irradiation time increased, Young's modulus increased for irradiation times up to 1 hour and beyond this time decreased slightly, with the tensile strength, strain at break, and work to break values, which is the energy required or work to break the sample, changing similarly. It is noted for an irradiation time of 3 hours, the samples showed a necking behavior similar to that observed in our previous study.[45] We suppose that

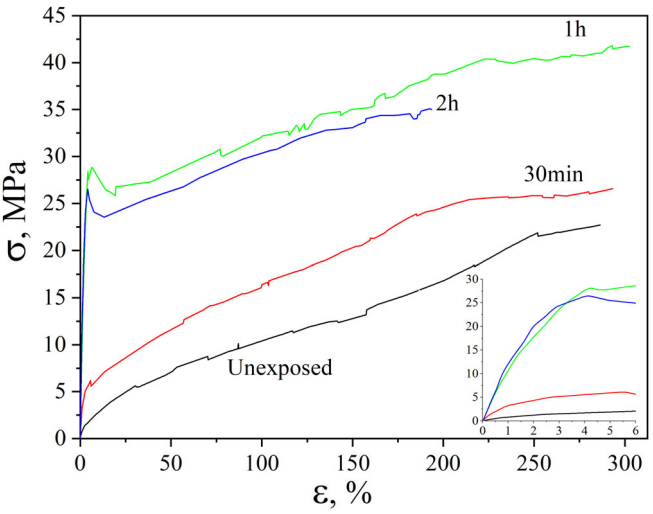


FIGURE 1 Influence of UV irradiation on the stress-strain curves of the pure PVA films. PVA, poly(vinyl alcohol); UV,ultraviolet [Color figure can be viewed at wileyonlinelibrary.com]

TABLE 1 Uniaxial tensile properties with SD of unexposed rGO/PVA composite films with varying wt% rGO content

Wt% rGO	E_Y, MPa	σ_T, MPa	ε_b, %	W_b, J
0	48.40 ± 12.66	20.73 ± 3.43	285.23 ± 87.38	0.160 ± 0.071
1	169.15 ± 41.91	24.95 ± 2.98	283.35 ± 22.54	0.418 ± 0.066
2.5	304.06 ± 69.80	24.99 ± 1.77	263.05 ± 48.96	0.335 ± 0.108
5	516.61 ± 58.26	22.40 ± 1.73	148.23 ± 18.46	0.208 ± 0.045
10	1067.29 ± 147.62	20.92 ± 0.61	43.71 ± 11.50	0.056 ± 0.025

Abbreviations: E_Y, Young's modulus; PVA, poly(vinyl alcohol); rGO, reduced graphene oxide; ε_b, strain at break; σ_T, tensile strength; W_b, work to break.

the necking formation in the stress-strain curves is due to combined effect of heating and UV irradiation. These changes in the tensile properties may be attributed to the effect of UV radiation which induces such chemical reactions in vinyl polymers as the formation of crosslinks, chain scission, and the formation of internal or terminal double bonds, as reported in prior studies.[20,46]

In the case of the rGO/PVA composite films, the UV irradiation significantly affected the stress-strain curves and the corresponding tensile properties of the films, as shown in Figure 2 and Table 3. Here, considerable changes were seen in the initial part of the stress-strain curves for all the rGO/PVA composite samples with increasing irradiation time. Obviously, a necking behavior was seen in the stress-strain curves for 1 and 2 hours irradiation and the stiffness of the samples was increased greatly. Although the tensile stress values at such low strain values as 4% to 5% increased greatly when compared with the value of the unexposed sample, as shown in Figure 2., the composite films dramatically lost their extensibility.

Table 3 shows how the uniaxial tensile characteristics changed depending on the UV irradiation time with increasing rGO loadings. Here, with the addition of rGO

TABLE 2 Uniaxial tensile properties with SD of pure PVA films irradiated by UV light for various times

UV irradiation time (h)	E_Y (MPa)	σ_T (MPa)	ε_b (%)	W_b (J)
0 (Unexposed)	48.40 ± 12.66	20.73 ± 3.43	285.23 ± 87.38	0.160 ± 0.071
0.5	308.63 ± 68.25	25.63 ± 4.33	293.76 ± 54.95	0.369 ± 0.114
1	1865.60 ± 689.49	42.18 ± 8.21	302.28 ± 43.70	0.615 ± 0.043
2	1544.09 ± 294.35	35.42 ± 4.65	195.10 ± 14.79	0.284 ± 0.042

Abbreviations: E_Y, Young's modulus; PVA, poly(vinyl alcohol); rGO, reduced graphene oxide; ε_b, strain at break; σ_T, tensile strength; UV, ultraviolet; W_b, work to break.

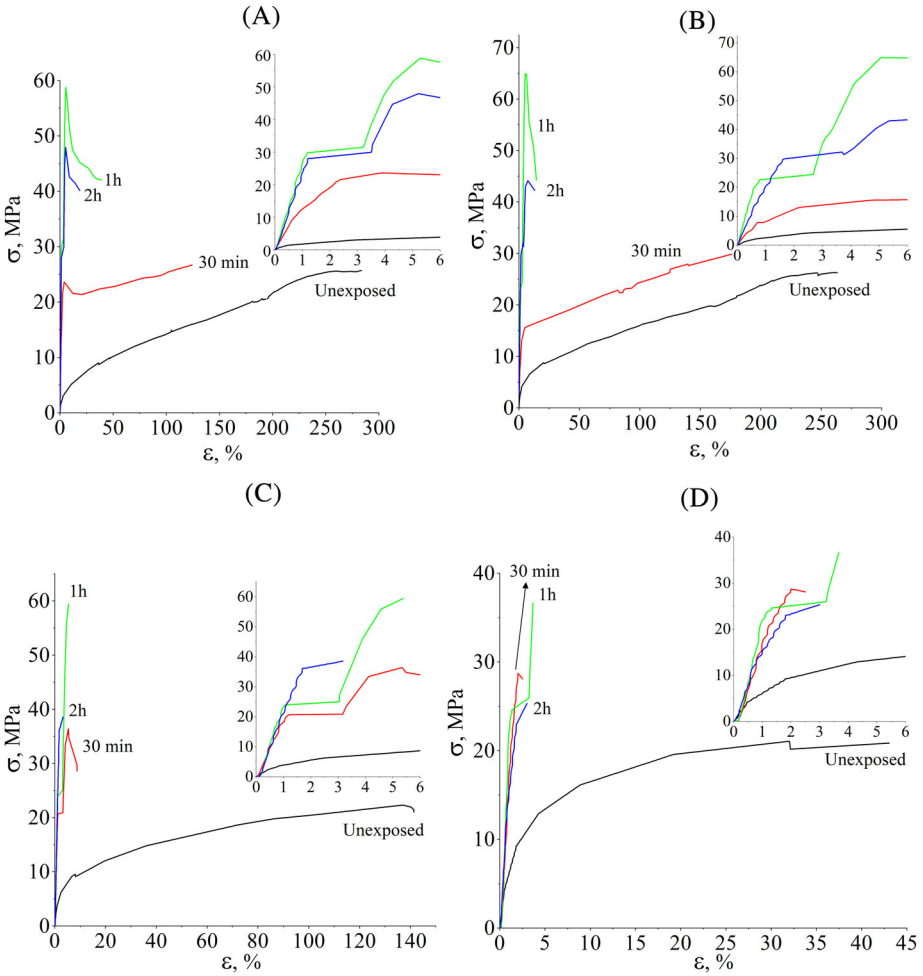


FIGURE 2 The influence of UV radiation for various times on the stress–strain curves of the rGO-PVA composite films: A, 1 wt% rGO-PVA; B, 2.5 wt% rGO-PVA; C, 5 wt% rGO-PVA; D, 10 wt% rGO-PVA. PVA, poly(vinyl alcohol); rGO, reduced graphene oxide; UV, ultraviolet [Color figure can be viewed at wileyonlinelibrary.com]

at all loadings, Young's moduli and tensile strength values were improved for irradiation times up to 1 hour and then decreased slightly. These increments in Young's modulus and tensile strength for 1% loading were almost 16 times and twice. Despite the significant increase in Young's modulus and thus the rigidity, the samples lost most of their extensibilities; thus, the strain at break values decreased dramatically for elevated irradiation times. A similar decrease was seen in the work to break values.

Figure 3 enables us to compare Young's modulus of the rGO-PVA composite films exposed to UV irradiation for the different times. It is seen that, in general, Young's modulus increased significantly for irradiation times up to 1 hour for each rGO-PVA film, independent of the rGO content. However, from the comparison of the values of Young's moduli in Figure 3 and Table 3 the ratio of Young's modulus values to that of the unexposed ones decreased from 16.49 to 2.97 as the rGO content was increased from 1 to 10 wt% for the irradiation time of 1 hour. Moreover, for the irradiation

TABLE 3 Uniaxial tensile properties with SD of the rGO/PVA composite films exposed to UV-radiation for various times

	UV Irradiation time (h)	E_Y (MPa)	σ_T (MPa)	*missent>/missent>*$_b$ (%)	W_b (J)
1 wt% rGO/PVA	0 (Unexposed)	169.15 ± 41.91	24.95 ± 2.98	283.35 ± 22.54	0.418 ± 0.066
	0.5	1768.29 ± 243.20	27.70 ± 2.43	124.48 ± 39.16	0.187 ± 0.076
	1	2787.44 ± 386.35	56.39 ± 4.19	39.23 ± 16.74	0.102 ± 0.050
	2	2040.28 ± 270.22	46.02 ± 4.85	20.4 ± 8.44	0.093 ± 0.044
2.5 wt% rGO/PVA	0 (Unexposed)	304.06 ± 69.80	24.99 ± 1.77	263.05 ± 48.96	0.335 ± 0.108
	0.5	1545.73 ± 462.27	32.45 ± 2.12	175.41 ± 29.94	0.339 ± 0.020
	1	3473.59 ± 458.65	66.15 ± 2.42	14.35 ± 3.30	0.047 ± 0.007
	2	2170.71 ± 296.47	43.38 ± 6.28	12.06 ± 4.21	0.022 ± 0.013
5 wt% rGO/PVA	0 (Unexposed)	516.61 ± 58.26	22.40 ± 1.73	148.23 ± 18.46	0.208 ± 0.045
	0.5	2289.04 ± 390.47	37.20 ± 3.42	9.70 ± 3.27	0.020 ± 0.006
	1	3386.98 ± 578.42	63.11 ± 8.86	5.37 ± 0.24	0.013 ± 0.001
	2	2278.33 ± 350.25	49.68 ± 16.27	5.43 ± 0.27 ???YÜKSEK	0.014 ± 0.001
10 wt% rGO/PVA	0 (Unexposed)	1067.29 ± 147.62	20.92 ± 0.61	43.71 ± 11.50	0.056 ± 0.025
	0.5	1657.03 ± 305.55	27.90 ± 1.61	2.53 ± 0.26	0.003 ± 0.001
	1	3168.40 ± 675.96	38.50 ± 9.65	3.82 ± 0.43	0.006 ± 0.001
	2	2233.92 ± 760.30	25.40 ± 4.99	2.43 ± 0.23 ???	0.004 ± 0.001

Abbreviations: E_Y, Young's modulus; PVA, poly(vinyl alcohol); rGO, reduced graphene oxide; ε_b, strain at break; σ_T, tensile strength; UV, ultraviolet; W_b, work to break.

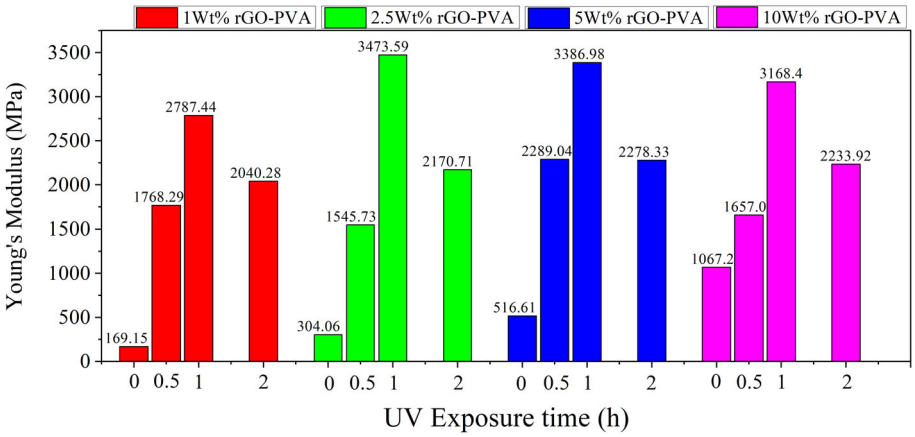


FIGURE 3 The influence of UV irradiation on Young's modulus of the rGO-PVA composite films. PVA, poly(vinyl alcohol); rGO, reduced graphene oxide; UV, ultraviolet [Color figure can be viewed at wileyonlinelibrary.com]

times higher than 1 hour, the modulus commonly decreased for all of the samples. Besides that, the film samples had higher levels of Young's modulus with increasing rGO content due to the reinforcing effect of the rGO content on the structure of the rGO-PVA composite films. Increased UV irradiation from 30 minutes to 1 hour also improved the stiffness and Young's modulus significantly. However, as shown in Table 3, as well as the significant effect of rGO content on decreasing the strain at break value of the unexposed rGO-PVA composite films, the UV irradiation reduced it more. Therefore, with the increasing UV irradiation time, the films became more brittle, losing most of their extensibilities and the other tensile properties due to the photodegradation of the film structure. Hence, the required energy or the work needed to break the composite films during the uniaxial extension decreased greatly for all the rGO loadings used. Furthermore, it is seen that regardless of the rGO content in the film samples, the ultimate tensile strength was improved significantly with increasing irradiation time up to 1 hour, and then it decreased considerably, also due to severe photodegradation. Here, although there is a heat effect due to increasing temperature up to around 40°C to 50°C during UV irradiation, because this can give only low thermal energy in the order of $kT \cong 2.4$ kJ mol^{-1} calculated for ambient temperature and cannot cause breakage in chemical bonds[46] which requires the dissociation energy in the order of 150-400 kJ per mol, this heating is considered to affect slightly the vibrational motion of molecules and give low thermal energy and thus, it can be negligible when compared with that of UV irradiation. It was also shown in our previous study[32] that heating rGO/PVA films at 50°C did not change tensile properties of the samples considerably and resulted in similar tensile characteristics and stress-strain behaviors to those of unheated samples.

Considering UV irradiation, it is known that depending on the wavelength or energy of the radiation, the UV radiation can have various effects on the polymer structure; that is, the photochemical reactions of vinyl polymers can vary from chain scissions, which can cause free radicals, to the formation of crosslinking and of some new bonds such as internal or terminal double bonds. Thus, we may attribute the reduced extensibility of the rGO-PVA composite films to the significant main chain scissions particularly in the amorphous PVA domains.

3.2 | FTIR/ATR and UV-vis spectral analysis

In order to investigate the interaction between the polymer matrix and the rGO sheets, the FTIR/ATR spectra of the pure PVA and rGO/PVA composites, as prepared, were analyzed. The spectra of some of the rGO/PVA composite films are shown in Figure 4 in the spectral range of 800-3700 cm^{-1}, each of which was vertically shifted for better illustration, before and after the composite films were irradiated for 30 minutes, 1 hour, and 2 hours. The spectra show the characteristic absorption bands of the pure PVA and the rGO/PVA composites before and after UV irradiation. In the spectra of PVA, the band at 1141 cm^{-1} is assigned to ν(C—C) stretching vibrations of the carbon framework of the polymer chain in the crystalline phase. Another band, at around 1088 cm^{-1}, is assigned to ν(C—) stretching vibrations.[47–53] The band at 1732 cm^{-1} corresponds to C═O stretching vibrations of the carbonyl groups, which are due to absorption by residual acetate groups due to the manufacture of PVA from hydrolysis by the polyvinyl acetate. This band has also been attributed to C═O stretching vibrations of the carbonyl groups at the edges of planes of graphite layers in the FTIR spectrum of GO.[24] In another important spectral region, 3000-3700 cm^{-1}, where intermolecular interactions between PVA and rGO sheets, such as hydrogen bonding, change significantly with the change or new formation of hydrogen bond interactions due to the additive rGO contents; the broad band at around 3100-3600 cm^{-1} can be assigned to the stretching vibrations of hydroxyl groups of mostly the PVA structure being either non-bonded or hydrogen bonded.[49–52,54–57] The band centered at 3280 cm^{-1} is ascribed to the stretching vibration of hydroxyl groups with strong hydrogen bonding in pure PVA films.[56,58,59] In some studies,[24,60–65] in the spectra of graphite and rGO, the peak appearing in the range of 3320-3430 cm^{-1} was also assigned to the C—OH stretching vibrations of a hydroxyl group. In our spectral region, this band was overlapped with the broad peak of OH groups of the PVA structure. Due to the effect of rGO content, the broadness and the absorbance value of the peak corresponding to OH stretching at around 3285 cm^{-1} changed.

In order to better understand how the structural changes occurred depending on both rGO content and UV irradiation time, the changes in the hydrogen bonding interactions and the crystallinity ratio in the polymer composites were determined by analyzing the obtained FTIR spectra in the range of 950-1800 and 2700-3600 cm^{-1}. In these spectral regions, the band at around 1141 cm^{-1} is known as a crystallization sensitive band[47,66] or crystallinity band.[53] The band at 1088 cm^{-1} is taken as a reference band for the calculation of the crystallinity ratio.[47–53] In order to calculate degree of crystallization, the areas of the peaks (1088 and 1144 cm^{-1}) were not resolved. Instead the absorbance intensities of these peaks by enlarging the spectral region of these peaks were used for the calculations.

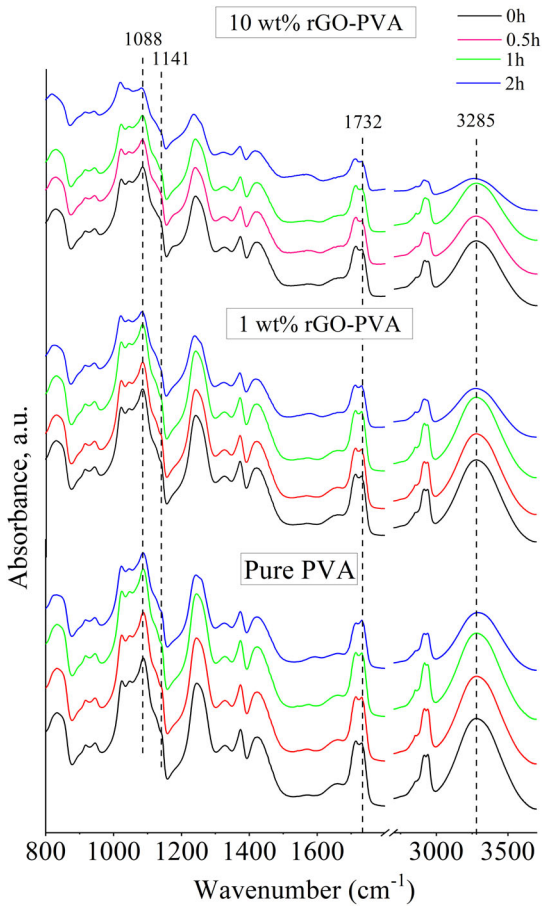


FIGURE 4 Fourier transform infrared/Attenuated total reflectance (FTIR/ATR) spectra of the pure PVA and rGO/PVA composite films exposed to UV radiation for various times. PVA (poly vinyl alcohol); rGO, reduced graphene oxide; UV, ultraviolet [Color figure can be viewed at wileyonlinelibrary.com]

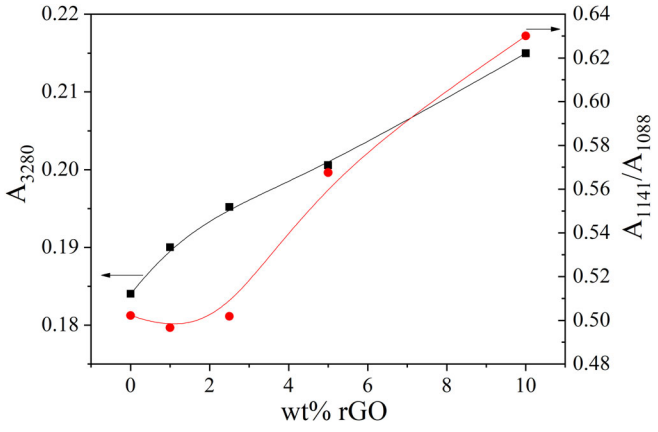


FIGURE 5 The changes in the absorbance (A_{3280}) of OH stretching of hydrogen bonded OH groups and crystallinity ratio (A_{1141}/A_{1088}) of unexposed rGO/PVA composite films with increasing wt% rGO content. PVA, poly(vinyl alcohol); rGO, reduced graphene oxide [Color figure can be viewed at wileyonlinelibrary.com]

This ratio permits determination of how the crystallinity of the rGO-PVA composite films changed. In Figure 5 a significant improvement in the crystallinity ratio due to the addition of the rGO sheets is seen; that is, the crystallinity ratio in the neat PVA film increased with increasing rGO content higher than around 2.5%. This is expected because the GO has been shown to act as crystallization nuclei of the PVA matrix.[24] Moreover, the absorbance of the hydrogen bonded OH stretching vibrations increased with increasing wt% rGO content, as also shown in Figure 5. It is known that there are oxygen-containing moieties such as carbonyl, carboxyl, hydroxyl, ether, and epoxy groups, on the surface of GO.[24] Because these groups can form hydrogen bonds with the OH groups of PVA molecules, the number of hydrogen-bonded OH groups increased significantly with increasing the rGO which significantly contributed to the increase in Young's modulus, tensile strength, and rigidity of the rGO/PVA composite films as discussed above.

Moreover, as shown in Figure 6, the absorbance of the C═O stretching vibrations of unirradiated rGO/PVA composite films at different rGO contents showed a similar change with increasing rGO content because rGO sheets have considerable carbonyl groups (C═O) which increase in number as the weight ratio of rGO to PVA was increased in the composite films. A general tendency of the absorbance of the C═O stretching vibrations is to increase with increasing the rGO content. Here, besides the formation of hydrogen bonding of some C═O groups, it is thought that some of the C═O groups do not participate in the formation of hydrogen bonding which leads to an increase in the absorbance of the C═O groups.

On the other hand, after the rGO/PVA composite films were irradiated by UV light for the different times,

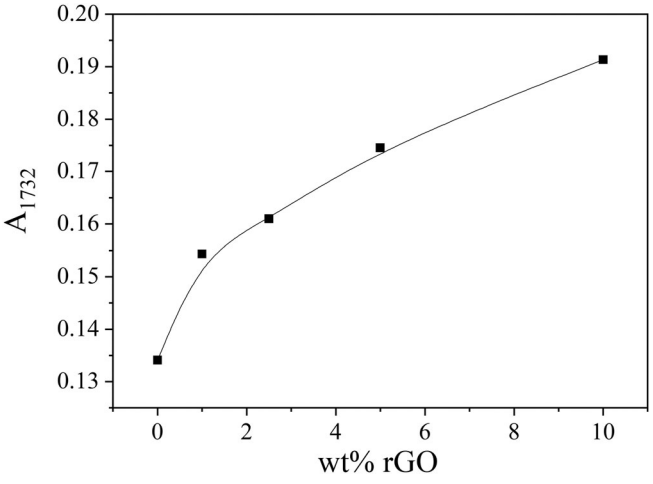


FIGURE 6 Change in the absorbance of C═O stretching of unexposed rGO/PVA composite films with respect to increasing wt % rGO content at room conditions

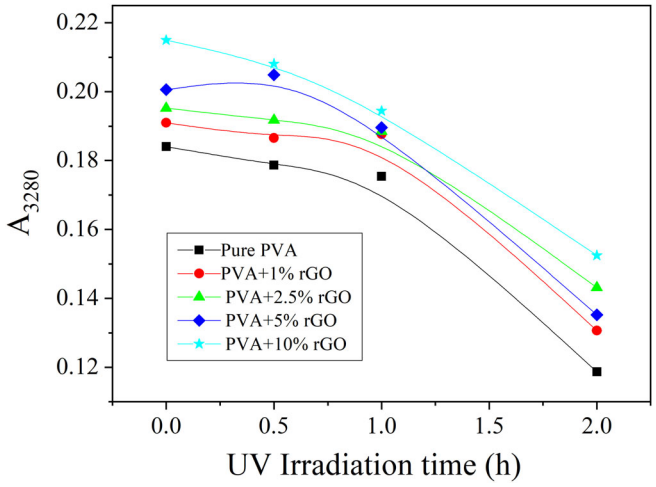


FIGURE 7 The absorbance ratio of the OH stretching vibrations of the hydrogen bonded OH groups of the pure PVA and rGO/PVA composite films for the different exposure times. PVA, poly(vinyl alcohol); rGO, reduced graphene oxide [Color figure can be viewed at wileyonlinelibrary.com]

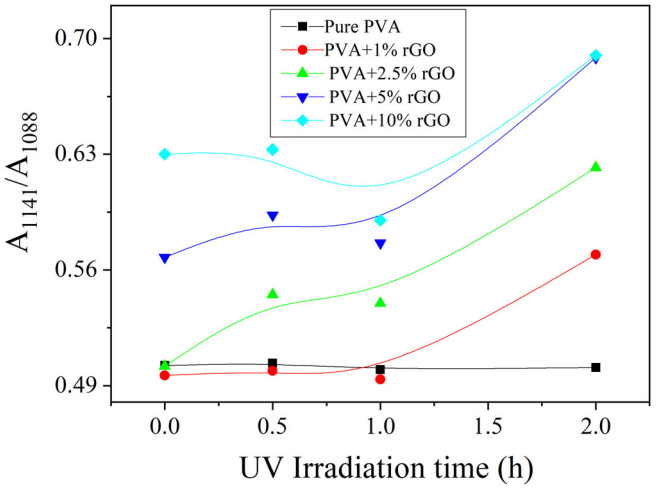


FIGURE 8 The crystallinity ratio (A_{1141}/A_{1088}) of the pure PVA and rGO/PVA composite films at different irradiation times. PVA, poly(vinyl alcohol); rGO, reduced graphene oxide [Color figure can be viewed at wileyonlinelibrary.com]

considerable changes were seen in the absorbance of the carbonyl groups stretching and hydrogen bonded OH groups vibrations, and the crystallinity ratio. Figure 7 shows the change in the absorbance ratio of the OH stretching vibrations of hydrogen bonded OH groups of the pure PVA and rGO/PVA composite films for the different irradiation times. The intensity of the band at 3280 cm^{-1} is affected by both intramolecular and/or intermolecular hydrogen bonds, which play an important key role for aggregation of the chains of many polymer molecules. As shown in Figure 7, the absorbance values for each specimen increased when the amount of rGO was increased because the rGO sheets are distributed in the polymer matrix and have more sites than those of pure PVA to form hydrogen bonds with PVA molecules. On the contrary, although the formation of hydrogen bonds did not change much for the low irradiation times up to around 1 hour, it decreased greatly for 2 hours irradiation time. Because UV radiation can cause photodegradation of the PVA via bond breakages in both the main chains and the side chains, for example, OH groups resulting in the formation of free radicals, in the creation of conjugated double bonds[24,25] some photodegradation products can form and intermolecular interactions, especially hydrogen bonds, can be easily broken during the photodegradation process. During this process, it was mentioned[67] that mainly OH groups on side chains undergo photochemical processes which lead to photooxidation of these groups or to the loss of water bonded to PVA film. Hence, similar to these results, the absorbance values of OH stretching group were reduced in our experimental findings (see Figure 7) as UV irradiation time increased. The photooxidation of OH groups and the formation of double bonds (C═C) change the intermolecular and intramolecular interactions and stability of the structure. Possible formation of double bonds makes the polymer chains more rigid and less extensible. Thus, these formation of double bonds in the main chains especially in amorphous regions which consists of more flexible and extensible polymer chains than those of ordered and crystalline regions restricted the extensibility of the polymer chains. In addition to the effect of reinforcing and rigidity effect of rGO sheets between PVA chains, new formation of such double bonds, other photo products, and some other weakening effect due to reaction by the UV irradiation can be assumed to be the main reasons for the decrease in the mechanical characteristics of the composite films, especially in the elongation at break.

In order to see the influence of the UV irradiation on the crystallinity ratio, the crystallinity ratios of the composite films with different rGO content with respect to UV irradiation times are shown in Figure 8. In general, the crystallinity ratio increased as the rGO contents in the PVA matrix were increased, as shown by the increasing level of the beginning points of the curves. For the pure PVA films the crystallinity ratio was almost constant and did not change with increasing irradiation time. However, the changing tendencies of the crystallinity ratio for the samples with the different the rGO doping ratios were similar to one another, the crystallinity ratio increasing sharply, especially for an irradiation time of 2 hours. While the irradiation time is increasing, even though the crystallinity ratio of pure PVA film did not

change considerably, the increasing tendency in the crystallinity ratio for each other curve may be caused by the dominant and improving effect of rGO sheets which interact with UV radiation and form stronger intermolecular interactions or some new chemical bonds during photodegradation process.

Figure 9 shows the changes in the absorbance of C═O stretching for all films as a function of irradiation time. The increasing absorbance level of the C═O stretching groups is caused by the increasing graphene content before the UV irradiation which is similar to the changing tendency of the absorbance ratio of the OH groups (Figure 7). Since intense photodegradation leads to various chemical bond breakages in different parts of the PVA chains, C═O containing groups and OH groups, from both the PVA and the GO sheets, can be broken. Hence, although the absorbance values for the films at different doping ratios were almost constant for shorter irradiation times up to 1 hour, it generally decreased for the irradiation time of 2 hours which is similar to the decrease in the absorbance of the H bonded OH groups as shown in Figure 7. However, with increasing rGO content up to 5%, the decrease rate of the absorbance value of the C═O stretching groups for the irradiation time from 1 to 2 hours was diminished, whereas the absorbance value increased for the 10 wt% rGO content in this time interval. We think that this increment effect is mainly due to the excessive amount of C═O containing groups of the rGO sheets for the 10 wt% rGO sample.

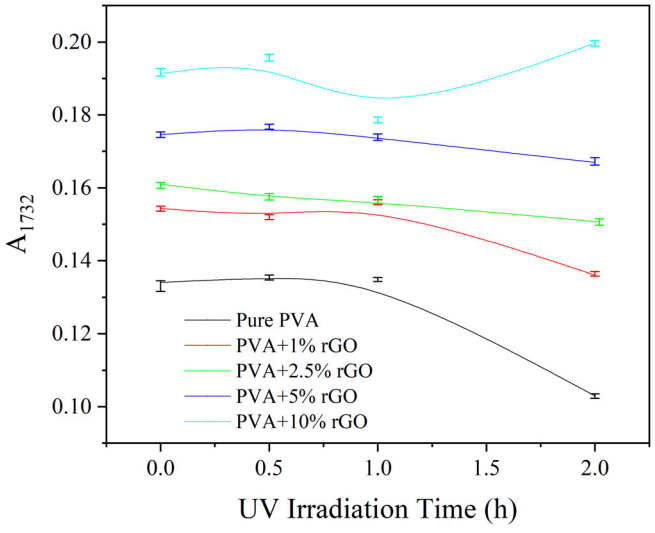


FIGURE 9 Change in the absorbance with SE bar of C═O stretching of the pure PVA and rGO/PVA composite films with respect to increasing irradiation time. PVA, poly(vinyl alcohol); rGO, reduced graphene oxide [Color figure can be viewed at wileyonlinelibrary.com]



FIGURE 10 Changing in the color with increasing rGO content: A, pure PVA; B, 2.5 wt% rGO/PVA; C, 5 wt% rGO/PVA; D, 10 wt% rGO/PVA for unexposed samples. PVA, poly(vinyl alcohol); rGO, reduced graphene oxide [Color figure can be viewed at wileyonlinelibrary.com]

The optical transparency and changes in the color of the composite films are important for the transmission of the light. As shown in Figure 10, the transparency of the films changed from transparent to opaque gradually with

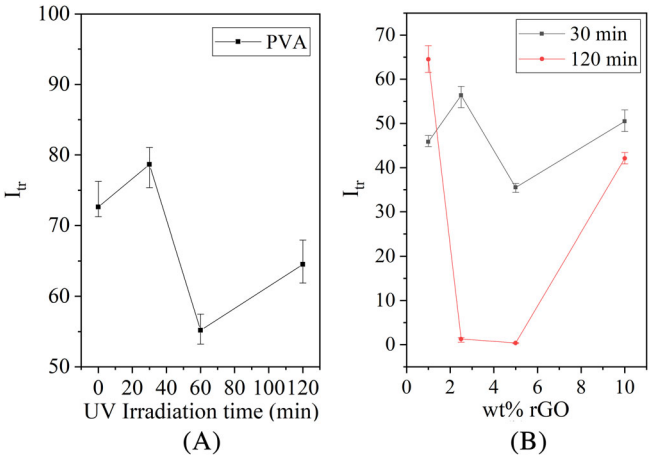
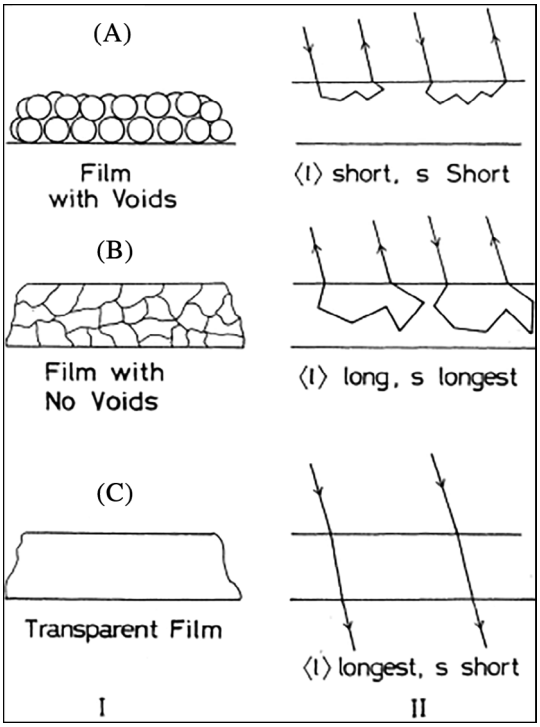


FIGURE 11 A, The change of the transmitted light intensity (I_{tr}) with SE bar through pure PVA for the different exposure times and, B, of I_{tr} from PVA and PVA/rGO composites exposed to UV irradiation of 30 and 120 minutes. PVA, poly(vinyl alcohol); rGO, reduced graphene oxide; UV, ultraviolet [Color figure can be viewed at wileyonlinelibrary.com]

increasing rGO content. As a result of this, the corresponding absorbance values in the UV-vis experiments increased as the rGO loading was increased. Using the results of the UV-vis spectroscopy, the change in the transmitted light intensity (I_{tr}) from the pure PVA films for the different irradiation times are shown in Figure 11A. I_{tr} increased for a UV irradiation time of 30 minutes, dropped for an exposure time of 60 minutes, and then increased for an exposure time of 120 minutes. This can be explained by the change in the morphology of the films.[68,69] These films were prepared without any substrate and could be easily affected by the UV irradiation. Relative to Figure 11A, it is thought that film surface expanded for an irradiation time of 30 minutes under heating due to the UV, hence, the film became more homogeneous which resulted in higher transmitted light intensity. For an irradiation time of 60 minutes, the film shrinks and then expands again for the irradiation time from 60 to 120 minutes. This shrunk surface scatters light while the expanding surface is opposite of it and these differences in the structures cause low and high I_{tr}, respectively.



SCHEME 1 I- Film formation process at different stages (A) Film with voids, (B) Film with no voids, (C) Transparent film; II- their variation in mean free ⟨l⟩ and optical paths ⟨s⟩

Figure 11B shows the change in I_{tr} with respect to the rGO content in the rGO/PVA composites for two different UV irradiation times. For the rGO contents of 2.5 and 5 wt% the films after 120 minutes irradiation were opaque, while for higher rGO rate, 10 wt%, an increase in transparency is seen in Figure 11B. These changes mean that the addition of rGO created new clusters which led to more voids for rGO ratios up to 5 wt% in the composite films. This results in a shorter mean free path of the light.

Film formation process and mean free and optical paths <*l*> and <*s*> are seen in Scheme 1. The first step of the film formation is shown in Scheme 1A, where a film which includes many voids. This film yields low I_{tr}. Scheme 1B presents a film where, due to annealing, interparticle voids start to disappear which gives rise to higher <*l*> and the longest <*s*> values. This results in

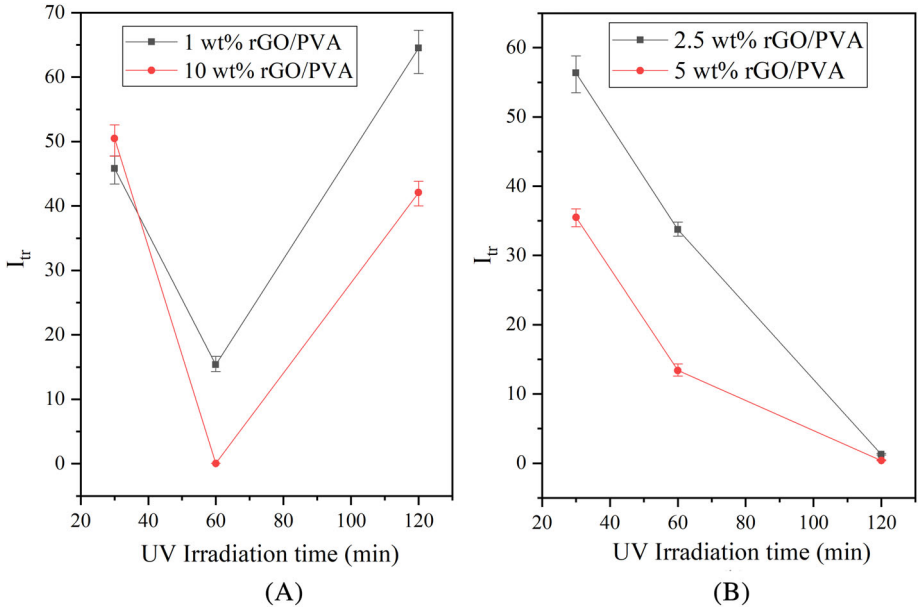


FIGURE 12 The variation of transmitted light intensity (I_{tr}) with SE bar with increasing UV irradiation times from rGO/PVA composite films: A, 1 wt % rGO/PVA and 10 wt% rGO/PVA; B, 2.5 wt% rGO/PVA and 5 wt% rGO/PVA. PVA, poly(vinyl alcohol); rGO, reduced graphene oxide [Color figure can be viewed at wileyonlinelibrary.com]

the higher I_{tr} intensity. Scheme 1C shows a homogeneous film with the longest <*l*> but smaller <*s*> values. This results in highest I_{tr} intensity.[70]

After this concentration rate (5%), the clusters start to move again and change their places of rGO and PVA. Due to this relocation, I_{tr} will become higher for the PVA distribution since its optical clarity. Although this decrease in I_{tr} cannot be seen very clearly in the films exposed to UV for 30 minutes, the general downward trend of up to 5% in I_{tr} is clearly seen especially at 120°C (see Figure 11B).

Figure 12 gives us an interesting information about the change of I_{tr}, that is, while it is first decreasing for the UV irradiation time up to 60 minutes and then increasing for the 1 wt% rGO/PVA and 10 wt% rGO/PVA composite films as seen in Figure 12A and it is continuously decreasing for the rGO content of 2.5 and 5 wt% in PVA matrix for the different irradiation times of the samples, as shown in Figure 12B. It is clearly understood that all the films were affected by the exposure time in terms of the change of I_{tr}. Decreasing of I_{tr} during 60 minutes of irradiation time for all of the samples can be firstly explained by the shrinking of the films accompanied by the deformation and degradation of the film surface due to the irradiation for this time interval for all the samples. It is known that the light intensity passing through the shrunken films is scattered more and causes a decrease in I_{tr}. Secondly, the aggregates formed in a composite matrix composed of the PVA and the rGO, which have different morphological structure, cause a decrease in I_{tr}. However, for the irradiation time higher than 60 minutes, I_{tr} increased for only pure PVA (see Figure 11A), 1 wt% rGO/PVA, and 10 wt% rGO/PVA composite films because the rGO clusters changed their places with the continuous addition of rGO up to 10 wt% which causes more homogeneity for instant and results in higher I_{tr}.

4 | CONCLUSIONS

Due to strong intermolecular interactions between the rGO sheets with the PVA polymer chains via the formation of hydrogen bonds, the reinforcement effects of the rGO on the tensile properties of pure PVA films such as tensile strength, rigidity, and Young's modulus were shown for the unirradiated rGO/PVA composite films as wells as pure PVA films. For instance, Young's modulus increased gradually for the rGO content from 1 to 5 wt% and then almost 22 times for higher rGO ratio of 10 wt%. Due to increasing rigidity, elongation at break values decreased greatly. After the samples were exposed to UV radiation, UV radiation-induced changes were seen on the uniaxial tensile and spectroscopic properties of rGO/PVA composite films. For the exposure time from minutes up to 1 hour, for all rGO contents, the rGO/PVA composite films obtained improved tensile strength and modulus values with a great decrease in strain at break value. However, after 1 hour of UV exposure time, with increasing influence of photodegradation in the composite film structure, a great decrease in the tensile properties such as strain at break value was seen. The decrease in the extensibility was caused by both the addition of the rGO content and UV induced-changes in crosslinking, and chain scission as a result of photodegradation of structural units induced by some free radicals formed by chemical bond breakages. It was also observed that the film formation properties were enhanced with the addition of the rGO above 5% content and the irradiation time above 60 minutes. Furthermore, the formation and/or breakage of intermolecular interactions such as hydrogen bonding between the rGO sheets and the PVA polymer chains through C═O and OH groups were shown by the changes in the absorbance value of OH groups by means of the FTIR/ATR spectral results. It can be said that the optimal composition that gives the best properties in terms of both mechanical and film formation is 5 wt% rGO-doped PVA exposed to 1 hour UV radiation. In addition, other spectroscopic and structural changes obtained in FTIR/ATR and UV-vis spectral results were used to comprehend the UV radiation-induced changes in the uniaxial tensile properties of the rGO/PVA composite films.

ACKNOWLEDGMENTS

The authors acknowledge the financial support of Scientific Research Projects Coordinatorship in Yıldız Technical University in Istanbul, Turkey, through the Grant of the Project with the number of 2016-01-01-GEP02.

ORCID

Altan Bozdoğan https://orcid.org/0000-0002-6493-0210
Baki Aksakal https://orcid.org/0000-0003-1255-541X
Onder Yargi https://orcid.org/0000-0001-6343-0057
Utkan Şahintürk https://orcid.org/0000-0002-1943-3450

REFERENCES

[1] J. Li, L. Shao, L. Yuan, Y. Wang, *Mater. Des.* **2014**, *54*, 520. https://doi.org/10.1016/J.MATDES.2013.08.090.
[2] Yang X, Li L, Shang S, Ming TX. *Polymer (Guildf).* **2010**;*51* (15):3431–3435. doi:https://doi.org/10.1016/j.polymer.2010.05.034
[3] M. J. McAllister, J. L. Li, D. H. Adamson, H. C. Schniepp, A. A. Abdala, J. Liu, M. Herrera-Alonso, D. L. Milius, R. Car, R. K. Prud'homme, I. A. Aksay, *Chem. Mater.* **2007**, *19*(18), 4396. https://doi.org/10.1021/cm0630800.
[4] C. Lee, X. Wei, J. W. Kysar, J. Hone, *Science* **2008**, *321*(5887), 385. https://doi.org/10.1126/science.1157996.

[5] X. Zhao, Q. Zhang, D. Chen, P. Lu, *Macromolecules* **2010**, *43* (5), 2357. https://doi.org/10.1021/ma902862u.

[6] G. Eda, M. Chhowalla, *Nano Lett.* **2009**, *9*(2), 814. https://doi.org/10.1021/n18035367.

[7] J. L. Vickery, A. J. Patil, S. Mann, *Adv. Mater.* **2009**, *21*(21), 2180. https://doi.org/10.1002/adma.200803606.

[8] K. M. Tripathi, F. Vincent, M. Castro, J. F. Feller, *Nanocomposites* **2016**, *2*(3), 125. https://doi.org/10.1080/20550324.2016.1227546.

[9] A. Begum, K. M. Tripathi, S. Sarkar, *Chem. A Eur. J.* **2014**, *20* (50), 16657. https://doi.org/10.1002/chem.201404461.

[10] G. S. Das, S. Sarkar, R. Aggarwal, S. K. Sonkar, J. W. Park, K. M. Tripathi, T. Y. Kim, *Carbon Lett.* **2019**, *29*(6), 595. https://doi.org/10.1007/s42823-019-00058-4.

[11] X. Wang, L. Zhi, K. Müllen, *Nano Lett.* **2008**, *8*(1), 323. https://doi.org/10.1021/nl072838r.

[12] J. D. Fowler, M. J. Allen, V. C. Tung, Y. Yang, R. B. Kaner, B. H. Weiller, *ACS Nano.* **2009**, *3*(2), 301. https://doi.org/10.1021/nn800593m.

[13] K. I. Bolotin, K. J. Sikes, Z. Jiang, M. Klima, G. Fudenberg, J. Hone, P. Kim, H. L. Stormer, *Solid State Commun.* **2008**, *146* (9–10), 351. https://doi.org/10.1016/J.SSC.2008.02.024.

[14] Y. Wang, Z. Shi, Y. Huang, Y. Ma, C. Wang, M. Chen, Y. Chen, *J. Phys. Chem. C.* **2009**, *113*(30), 13103. https://doi.org/10.1021/jp902214f.

[15] M. El Achaby, A. Qaiss, *Mater Des.* **2013**, *44*, 81. https://doi.org/10.1016/J.MATDES.2012.07.065.

[16] M. Liang, L. Zhi, *J. Mater. Chem.* **2009**, *19*(33), 5871. https://doi.org/10.1039/b901551e.

[17] J. Geng, L. Liu, S. B. Yang, S. C. Youn, D. W. Kim, J. S. Lee, J. K. Choi, H. T. Jung, *J. Phys. Chem. C.* **2010**, *114*(34), 14433. https://doi.org/10.1021/jp105029m.

[18] L. Shen, H.-S. Shen, C.-L. Zhang, *Mater. Des.* **2010**, *31*(9), 4445. https://doi.org/10.1016/J.MATDES.2010.04.016.

[19] R. Verdejo, M. M. Bernal, L. J. Romasanta, M. A. Lopez-Manchado, *J. Mater. Chem.* **2011**, *21*(10), 3301. https://doi.org/10.1039/C0JM02708A.

[20] K. M. Abd El-Kader, A. Y. M. El-Lawindy, A. F. Mansour, S. F. Abdel Hamied, *J. Appl. Polym. Sci.* **2002**, *84*(6), 1295. https://doi.org/10.1002/app.10486.

[21] M. I. Baker, S. P. Walsh, Z. Schwartz, B. D. Boyan, *J. Biomed. Mater. Res. B Appl. Biomater.* **2012**, *100B*(5), 1451. https://doi.org/10.1002/jbm.b.32694.

[22] C. DeMerlis, D. Schoneker, *Food Chem. Toxicol.* **2003**, *41*(3), 319. https://doi.org/10.1016/S0278-6915(02)00258-2.

[23] S. Mahendia, K. G. Heena, U. P. Deshpande, S. Kumar, *J. Mol. Struct.* **2016**, *1111*, 46. https://doi.org/10.1016/J.MOLSTRUC.2016.01.072.

[24] S. Morimune, T. Nishino, T. Goto, *Polym. J.* **2012**, *44*(10), 1056. https://doi.org/10.1038/pj.2012.58.

[25] T. Cheng-an, Z. Hao, W. Fang, Z. Hui, Z. Xiaorong, W. Jianfang, *Polym. Polym. Compos.* **2017**, *25*(1), 11. https://doi.org/10.1177/096739111702500102.

[26] S. G. Rathod, R. F. Bhajantri, V. Ravindrachary, P. K. Pujari, T. Sheela, J. Naik, Thermal, mechanical and dielectric properties of poly(vinyl alcohol)/graphene oxide composites. in *AIP Conf. Proc.*, American Institute of Physics, Punjab, India, **2014**, 1591, 1769. https://doi.org/10.1063/1.4873107.

[27] J. Liang, Y. Huang, L. Zhang, Y. Wang, Y. Ma, T. Guo, Y. Chen, *Adv. Funct. Mater.* **2009**, *19*(14), 2297. https://doi.org/10.1002/adfm.200801776.

[28] O. C. Compton, S. W. Cranford, K. W. Putz, Z. An, L. C. Brinson, M. J. Buehler, S. B. T. Nguyen, *ACS Nano.* **2012**, *6*(3), 2008. https://doi.org/10.1021/nn202928w.

[29] Y. Xu, W. Hong, H. Bai, C. Li, G. Shi, *Carbon* **2009**, *47*(15), 3538. https://doi.org/10.1016/J.CARBON.2009.08.022.

[30] L. Liu, Y. Gao, Q. Liu, J. Kuang, D. Zhou, S. Ju, B. Han, Z. Zhang, *Small.* **2013**, *9*(14), 2466. https://doi.org/10.1002/smll.201300819.

[31] Q. Bian, H. Tian, Y. Wang, Q. Liu, X. Ge, A. V. Rajulu, A. Xiang, *Polym. Sci. Ser. A* **2015**, *57*(6), 836. https://doi.org/10.1134/S0965545X15060048.

[32] A. Bozdoğan, B. Aksakal, U. Şahintürk, Ö. Yargı, *J. Mol. Struct.* **2018**, *1174*, 133. https://doi.org/10.1016/j.molstruc.2018.06.011.

[33] S. P. Vijayalakshmi, G. Madras, *J. Appl. Polym. Sci.* **2006**, *102* (2), 958. https://doi.org/10.1002/app.23736.

[34] B. G. Rånby, J. F. Rabek, *ESR Spectroscopy in Polymer Research*, Springer-Verlag, Berlin; New York **1977**.

[35] G. Rudko, A. Kovalchuk, V. Fediv, W. M. Chen, I. A. Buyanova, *Nanoscale Res. Lett.* **2015**, *10*(1), 81. https://doi.org/10.1186/s11671-015-0787-5.

[36] Y. Chen, Z. Sun, Y. Yang, Q. Ke, *J. Photochem. Photobiol. A Chem.* **2001**, *142*(1), 85. https://doi.org/10.1016/S1010-6030(01)00477-4.

[37] H. Kaczmarek, A. Podgórski, *J. Photochem. Photobiol. A Chem.* **2007**, *191*(2–3), 209. https://doi.org/10.1016/j.jphotochem.2007.04.025.

[38] E. Baimuratov, D. S. Saidov, I. Y. Kalontarov, *Polym. Degrad. Stab.* **1993**, *39*(1), 35. https://doi.org/10.1016/0141-3910(93)90122-Y.

[39] S. P. Vijayalakshmi, G. Madras, *J. Appl. Polym. Sci.* **2006**, *100* (6), 4888. https://doi.org/10.1002/app.23280.

[40] S. P. Vijayalakshmi, G. Madras, *J. Appl. Polym. Sci.* **2006**, *101* (1), 233. https://doi.org/10.1002/app.23246.

[41] H. Aoki, M. Uehara, T. Suzuki, A. Yoshida, *Eur. Polym. J.* **1980**, *16*(7), 571. https://doi.org/10.1016/0014-3057(80)90089-0.

[42] J. M. De Souza, P. N. M. Dos Anjos, E. C. Pereira, Y. G. Gobato, L. S. Dos Santos, *Synth. Met.* **2002**, *130*(2), 121. https://doi.org/10.1016/S0379-6779(02)00118-2.

[43] D. Akyüz, B. Keskin, U. Şahintürk, A. Koca, *Appl. Catal. B Environ.* **2016**, *188*, 217. https://doi.org/10.1016/J.APCATB.2016.02.003.

[44] H. Berber, E. Ucar, U. Sahinturk, *Coll. Surf. A Physicochem. Eng. Asp.* **2017**, *531*, 56. https://doi.org/10.1016/J.COLSURFA.2017.07.057.

[45] B. Aksakal, Ö. Yargı, U. Şahinturk, *J. Appl. Polym. Sci.* **2017**, *134*(23), 44915. https://doi.org/10.1002/app.44915.

[46] W. Schnabel, *Polymer Degradation: Principles and Practical Applications*, Hanser International, Illustrated edition. Munchen, Wien **1981**. https://trove.nla.gov.au/work/15349337?q&versionId=32443048+228623347 (accessed: September 24, 2019).

[47] A. M. Shehap, *Egypt J. Solids* **2008**, *31*(1), 75. https://pdfs.semanticscholar.org/e373/1ceeadd22c9ca3286d27ec69426f52eb5ced.pdf (accessed: March 25, 2019).

[48] C. L. Raju, J. L. Rao, B. C. V. Reddy, B. K. Veera, *Bull. Mater. Sci.* **2007**, *30*(3), 215. https://doi.org/10.1007/s12034-007-0038-1.

[49] J. Ahmad, K. Deshmukh, M. B. Hägg, *Int. J. Polym. Anal. Charact.* **2013**, *18*(4), 287. https://doi.org/10.1080/1023666X.2013.767080.

[50] M. Tsukada, G. Freddi, J. S. Crighton, *J. Polym. Sci. B Polym. Phys.* **1994**, *32*(2), 243. https://doi.org/10.1002/polb.1994.090320205.

[51] E. A. El-Hefian, M. M. Nasef, A. H. Yahaya, *E J. Chem.* **2011**, *8*(1), 91. https://doi.org/10.1155/2011/969062.

[52] W. A. Jabbar, N. F. Habubi, S. S. Chiad, *J. Ark. Acad Sci.* **2010**, *64*, 101. http://scholarworks.uark.edu/jaashttp://scholarworks.uark.edu/jaas/vol64/iss1/21 (accessed: March 25, 2019).

[53] O. N. Tretinnikov, S. A. Zagorskaya, *J. Appl. Spectrosc.* **2012**, *79*, 521. https://link.springer.com/content/pdf/10.1007%2Fs10812-012-9634-y.pdf (accessed: March 25, 2019).

[54] I. Korbag, S. S. Mohamed, *Int. J. Environ. Stud.* **2016**, *73*(2), 226. https://doi.org/10.1080/00207233.2016.1143700.

[55] S. Krimm, C. Y. Liang, G. B. B. M. Sutherland, *J. Polym. Sci.* **1956**, *22*(101), 227. https://doi.org/10.1002/pol.1956.1202210106.

[56] P. Sakellariou, A. Hassan, R. C. Rowe, *Colloid. Polym. Sci.* **1993**, *271*(11), 1083. https://doi.org/10.1007/BF00659298.

[57] N. B. Rithin Kumar, V. Crasta, R. F. Bhajantri, B. M. Praveen, *J. Polym.* **2014**, *2014*, 1. https://doi.org/10.1155/2014/846140.

[58] G. Attia, M. F. H. Abd El-Kader, *Int. J. Electrochem. Sci.* **2013**, *8*, 5672. www.electrochemsci.org (accessed: March 25, 2019).

[59] K. S. Chan, H. B. Senin, I. Naimah, M. Rusop, T. Soga, Structural and mechanical properties of polyvinyl alcohol (PVA) thin film. in *AIP Conf. Proc.*, Vol. 1136, AIP, Selandor, Malaysia, **2009**, p. 366. https://doi.org/10.1063/1.3160165.

[60] S. Drewniak, R. Muzyka, A. Stolarczyk, T. Pustelny, M. Kotyczka-Morańska, M. Setkiewicz, *Sensors* **2016**, *16*(1), 103. https://doi.org/10.3390/s16010103.

[61] X. Yang, L. Ma, S. Wang, Y. Li, Y. Tu, X. Zhu, *Polymer (Guildf).* **2011**, *52*(14), 3046. https://doi.org/10.1016/J.POLYMER.2011.04.062.

[62] C. Hontoria-Lucas, A. J. López-Peinado, J. López-González, D. de Rojas-Cervantes, M. L. Rojas-Cervantes, R. M. Martín-Aranda, *Carbon NY* **1995**, *33*(11), 1585. https://doi.org/10.1016/0008-6223(95)00120-3.

[63] S. Y. Toh, K. S. Loh, S. K. Kamarudin, W. R. W. Daud, *Chem Eng J.* **2014**, *251*, 422. https://doi.org/10.1016/J.CEJ.2014.04.004.

[64] C. Wang, Q. Jin, Y. Wang, H. Yin, H. Xie, R. Cheng, *Mater Lett.* **2012**, *68*, 280. https://doi.org/10.1016/J.MATLET.2011.10.088.

[65] W. J. Kim, C. Basavaraja, P. X. Thinh, D. S. Huh, *Mater Lett.* **2013**, *90*, 14. https://doi.org/10.1016/J.MATLET.2012.09.007.

[66] J. F. Kenney, G. W. Willcockson, *J. Polym. Sci. A Polym. Chem.* **1966**, *4*(3), 679. https://doi.org/10.1002/pol.1966.150040321.

[67] A. Sionkowska, A. Płanecka, J. Kozłowska, J. Skopińska-Wiśniewska, *Polym. Degrad. Stab.* **2009**, *94*(3), 383. https://doi.org/10.1016/j.polymdegradstab.2008.11.020.

[68] O. Yargi, A. Gelir, U. Sahinturk, T. Ozer, M. Caliskan, B. Aksakal, *Polym. Compos.* **2019**, *40*(S2), E1441. https://doi.org/10.1002/pc.25045.

[69] Ş. Uğur, Y. Kışlak, *Polym. Compos.* **2012**, *33*(8), 1274. https://doi.org/10.1002/pc.22252.

[70] Ş. Uğur, A. Alemdar, Ö. Pekcan, *Polym. Compos.* **2006**, *27*(3), 299. https://doi.org/10.1002/pc.20187.

How to cite this article: Bozdoğan A, Aksakal B, Yargi O, Şahintürk U. Structural and tensile characteristics of reduced graphene oxide/poly (vinyl alcohol) composite films: Influence of ultraviolet irradiation. *Polymer Composites*. 2020; 1–14. https://doi.org/10.1002/pc.25600